DOI: 10.1002/ejic.200500812

Polar Cofacially Fixed Sandwich Complexes: Do They Demonstrate Second Harmonic Generation (SHG)?

Maik Malessa,[a] Jürgen Heck,*[a] Jürgen Kopf,[a] and M. Helena Garcia[b]

Dedicated to Prof. Dr. Wittko Francke on the occasion of his 65th birthday

Keywords: Heterometallic complexes / Sandwich complexes / Donor–acceptor systems / Nonlinear optics / Through-space interaction

For the purpose of possible second harmonic generation (SHG) a cationic and a neutral sandwich unit were cofacially arranged in a three-step synthesis starting from 1,8-diiodonaphthalene. First, 1-cyclopentadienyl-8-iodonaphthalene (**2**) was formed, then the neutral ferrocenyl substituent was fixed in the 8-position by a Negishi cross-coupling reaction. The deprotonation of the cyclopentadienyl substituent, and the subsequent coordination of the half-sandwich fragments ML = $[Fe(\eta^5\text{-}C_5Me_5)]^+$, $[Rh(\eta^5\text{-}C_5Me_5)]^{2+}$, $[Ir(\eta^5\text{-}C_5Me_5)]^{2+}$, $[Ru(\eta^6\text{-}C_6H_6)]^{2+}$ to the cyclopentadienyl anion revealed the desired dinuclear complexes 1-[(η^5-cyclopentadienediyl)-(η^5-pentamethylcyclopentadienyl)iron(II)]-8-ferrocenylnaphthalene (**5**), 1-[(η^5-cyclopentadienediyl)(η^5-pentamethylcyclopentadienyl)rhodium(III)]-8-ferrocenylnaphthalene hexafluorophosphate (**6**PF_6), 1-[(η^5-cyclopentadienediyl)(η^5-pentamethylcyclopentadienyl)iridium(III)]-8-ferrocenylnaphthalene hexafluorophosphate (**7**PF_6), and 1-[(η^6-benzene)(η^5-cyclopentadienediyl)ruthenium(II)]-8-ferrocenylnaphthalene hexafluorophosphate (**8**PF_6). The neutral complex **5** was oxidized to the paramagnetic cation 1-[(η^5-cyclopentadienediyl)-(η^5-pentamethylcyclopentadienyl)iron(III)]-8-ferrocenylnaphthalene hexafluorophosphate (**5**PF_6). Compounds **3**, **5**PF_6, **6**PF_6, and **7**PF_6 were characterized by X-ray structure determination; the neutral compound **3** crystallizes in the space group $P2_1/c$, whereas all of the cationic dinuclear complexes crystallize in the chiral space group $C222_1$. A cyclic voltammetry study points to a predominant "through-space" interaction between the cationic sandwich unit and the neutral ferrocene substituent. The compounds **5**PF_6, **6**PF_6, **7**PF_6, and **8**PF_6 were subjected to hyper-Rayleigh scattering (HRS) and Kurtz-powder measurements. In both studies no SHG intensity could be observed.

Introduction

Cofacially stacked arrays of organic and organometallic π-systems are of increasing interest for chemists and physicists, because of novel electrical,[1,2] optical,[2] and magnetic[3] properties. Just recently, theoretical[4] and experimental[5] work has demonstrated that stacked donor–acceptor arrangements of π-systems are suitable for second harmonic generation (SHG) effected by through-space (hyper)polarization (Figure 1).

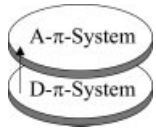

Figure 1. Cofacially stacked arrangement of donor(D)–acceptor(A) π-systems for second harmonic generation (SHG) due to polar "through-space" interaction.

Conventional types of compounds revealing nonlinear optical (NLO) properties, i.e. SHG, are composed of donor and acceptor units linked by conjugated π-bonds, which very often suffer from absorbance in the region of the SHG, and are thus not suitable for practical applications. In contrast, π-stacked donor-acceptor combinations seem to provide a better optical transparency.[6] Our approach to stacked organometallic π-complexes with donor–acceptor combinations, which may call forth SHG, is based on Rosenblum's concept of 1,8-disubstituted naphthalene derivatives containing two sandwich complexes in the *peri* position. Whereas the Rosenblum naphthalene derivatives are symmetrically constructed with the same sandwich complexes in the *peri* position,[7,8] our desired target molecules should contain different sandwich complexes,[9] one of which is a cation, generating an overall dipole moment, which is a possible prerequisite for SHG (Figure 2).

[a] Institut für Anorganische und Angewandte Chemie, Universität Hamburg,
Martin-Luther-King-Platz 6, 20146 Hamburg
[b] Faculdade de Ciências da Universidade de Lisboa, Ed. C8, Campo Grande, 1749-016 Lisboa, Portugal

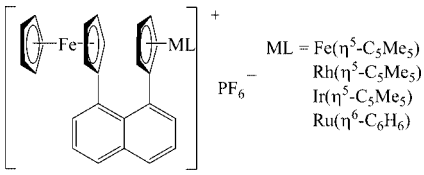

Figure 2. Unsymmetrically 1,8-disandwich-substituted naphthalene derivatives.

Results and Discussion

Synthesis

The assembly of different sandwich complexes in *peri* position of naphthalene requires a stepwise synthesis. Starting with a cross-coupling reaction of 1,8-diiodonaphthalene (**1**) [10] with cyclopentadienylzinc chloride[7a,9a] (Scheme 1), results in the formation of 1-cyclopentadienyl-8-iodonaphthalene (**2**). For the second step, a Pd-catalyzed Negishi cross-coupling reaction with ferrocenylzinc chloride[11,12] was performed, revealing complex **3**, which is composed of the two different isomers **3a** and **3b** (see Exp. Sect.). In order to synthesize the unsymmetrical disandwich-substituted naphthalene derivatives, complex **3** was subjected to a deprotonation by sodium bis(trimethylsilyl)amide to yield **4**, and a consecutive coordination reaction with the proper half-sandwich complexes (Scheme 1). For Rh, Ir, and Ru complexes **6**PF_6, **7**PF_6, and **8**PF_6, the deprotonated complex **4** was treated with thallium chloride in acetonitrile to replace the counterion Na^+ with Tl^+.[13] This cation exchange is necessary to obtain good yields of the desired dinuclear cationic complexes with Ru, Rh and Ir. In order to achieve the polar structure of the diiron derivative, compound **5** was oxidized to the paramagnetic monocation **5**PF_6 by addition of a stoichiometric amount of ferrocenium hexafluorophosphate (Scheme 2), and a dark red-brown crystalline material was obtained. All compounds were fully characterized by elemental analyses, spectroscopic methods and cyclic voltammetry. For compound **3a**, **5**PF_6, **6**PF_6 and **7**PF_6 X-ray structure analyses were determined.

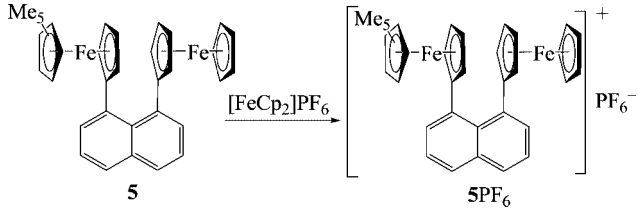

Scheme 2. Oxidation of **5** with ferrocenium hexafluorophosphate.

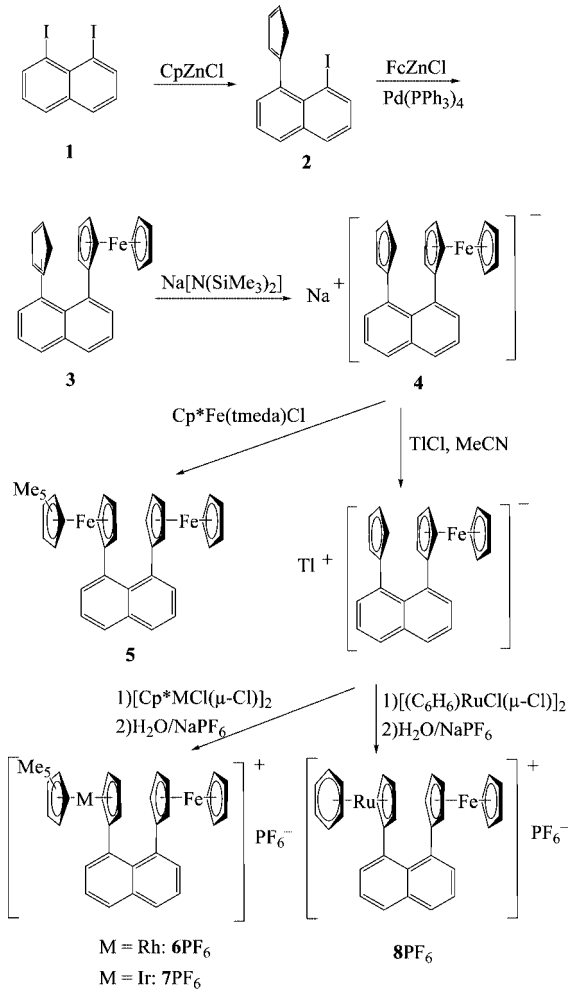

Scheme 1. Synthesis of polar cofacially fixed sandwich complexes.

Crystal Structures

The solid-state structures of **3a**, **5**PF_6, **6**PF_6 and **7**PF_6 are displayed in Figures 3, 4, 5 and 6. The mononuclear complex **3a** crystallizes in the monoclinic space group $P2_1/c$, whereas the space group for the dinuclear monocationic species is found to be orthorhombic and chiral with $C222_1$. Not surprisingly, the structural data of the sandwich units are very similar to those of published data for corresponding prototype sandwich complexes (Table 1).[14–17]

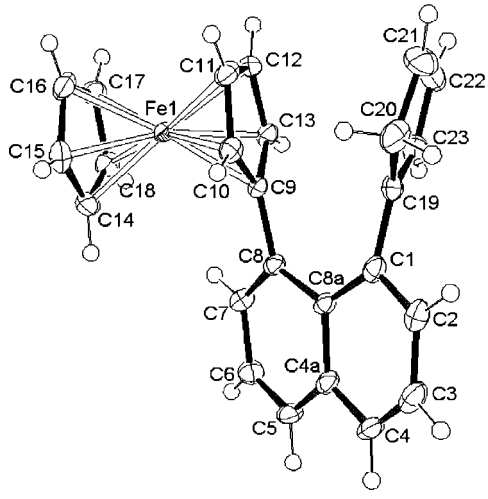

Figure 3. Molecular structure of **3a** (50% ellipsoids).

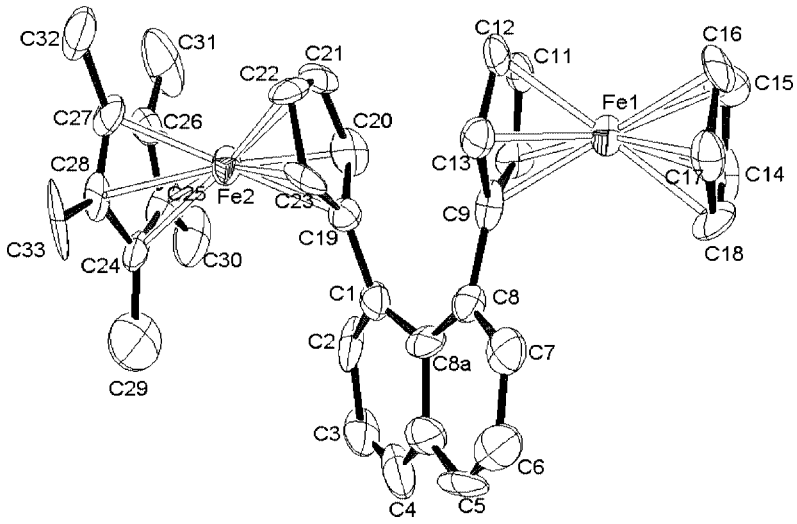

Figure 4. Molecular structure of **5**PF_6 (50% ellipsoids, hydrogen atoms and counterion are omitted for clarity).

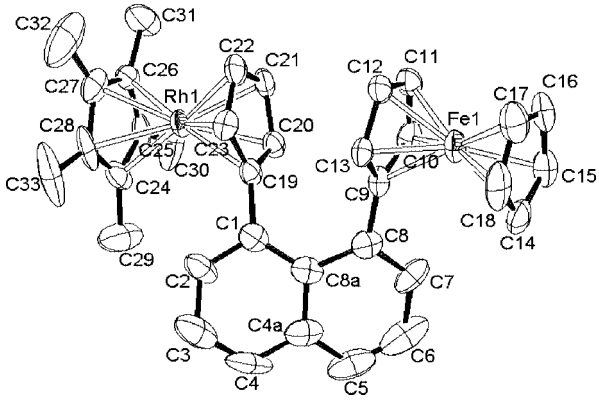

Figure 5. Molecular structure of **6**PF_6 (50% ellipsoids, hydrogen atoms and counterion are omitted for clarity).

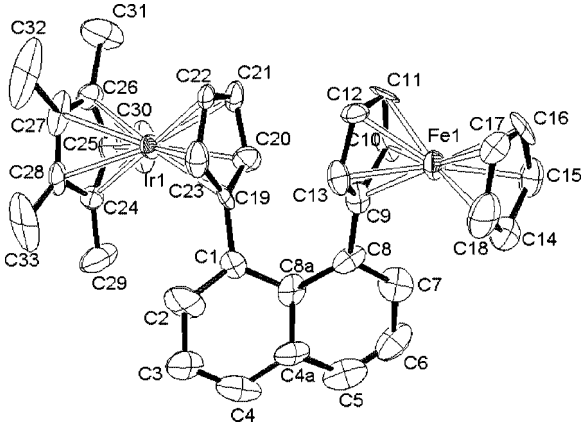

Figure 6. Molecular structure of **7**PF_6 (50% ellipsoids, hydrogen atoms and counterion are omitted for clarity).

Table 1. Selected bond lengths [pm] of the metallocene units in **3a**, **5**PF_6, **6**PF_6, **7**PF_6.

	3a	**5**PF_6	**6**PF_6	**7**PF_6
Fe(1)–C(9)	207.8(3)	206(1)	208(1)	208(2)
Fe(1)–C(10)	204.8(3)	205(1)	206(1)	204(3)
Fe(1)–C(11)	203.7(4)	203(1)	205(1)	201(3)
Fe(1)–C(12)	204.0(4)	204(1)	204(1)	201(2)
Fe(1)–C(13)	204.5(3)	206(1)	203(1)	204(2)
Fe(1)–$Cent_{[C(9)–C(13)]}$[a]	164.47(18)	165(1)	166(1)	165(1)
Fe(1)–C(14)	203.8(4)	204(2)	206(1)	206(3)
Fe(1)–C(15)	203.9(4)	202(2)	204(1)	210(2)
Fe(1)–C(16)	205.3(4)	205(2)	204(1)	203(3)
Fe(1)–C(17)	204.8(3)	204(1)	205(2)	208(2)
Fe(1)–C(18)	204.7(4)	205(1)	204(1)	203(3)
Fe(1)–$Cent_{[C(14)–C(18)]}$[a]	165.0(2)	166(1)	165(1)	168(1)
M–C(19)	–	215(1)	224(1)	219(2)
M–C(20)	–	207(2)	221(1)	217(3)
M–C(21)	–	206(2)	215(1)	219(2)
M–C(22)	–	205(1)	214(1)	217(2)
M–C(23)	–	210(1)	218(1)	220(2)
M–$Cent_{[C(19)–C(23)]}$[a]	–	171(1)	181(1)	183(1)
M–C(24)	–	210(2)	219(1)	215(3)
M–C(25)	–	210(2)	217(1)	224(3)
M–C(26)	–	202(2)	215(1)	220(3)
M–C(27)	–	207(2)	217(1)	218(2)
M–C(28)	–	217(2)	221(1)	220(3)
M–$Cent_{[C(24)–C(28)]}$[a]	–	170(1)	181(1)	182(1)
C(19)–C(20)	141.9(6)	144(2)	144(1)	139(3)
C(20)–C(21)	148.1(7)	139(2)	143(2)	146(4)
C(21)–C(22)	142.0(8)	140(2)	140(2)	133(3)
C(22)–C(23)	141.4(7)	142(2)	140(2)	145(3)
C(23)–C(19)	140.7(6)	137(2)	144(2)	143(3)
C(24)–C(25)	–	147(3)	143(2)	148(4)
C(25)–C(26)	–	137(2)	143(2)	146(5)
C(26)–C(27)	–	139(2)	141(2)	139(4)
C(27)–C(28)	–	145(2)	144(2)	144(4)
C(28)–C(24)	–	143(2)	143(2)	141(5)

[a] Cent: centroid of the corresponding cyclopentadienyl rings.

The most eye-catching feature of all structures under study is the distortion of the compound entities (Figure 7, Table 2); a common occurrence for naphthalene derivatives disubstituted in the 1,8-positions by aromatic moieties.[8,18] The tilt angle between the best plane of the naphthalene-bound Cp ligands and the best planes of the connected six-membered naphthalene rings varies from 45.6(6)° (**5**PF_6) to 77.9(8)° (**6**PF_6) (Table 2). For the less crowded example **3a**, with only one sandwich unit, intermediate tilt angles of 53.5(2)° and 53.0(2)° are found. Remarkably, the permethylation of one of the distal Cp ligands in the cationic species

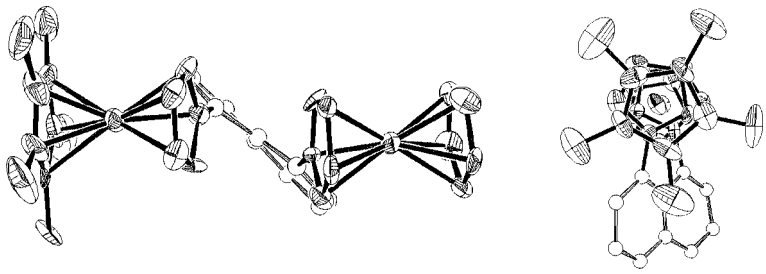

Figure 7. Cofacial arrangement of metallocene fragments in **5**PF_6; left: showing the interplanar distortion between the naphthalene moiety and the sandwich units; right: view along the metallocene axes; (50% ellipsoids, hydrogen atoms and counterion are omitted for clarity).

Table 2. Selected interplanar und torsion angles [°], bond lengths and interatomic distances [pm] between the naphthalene und metallocene units.

	3a	**5**PF_6	**6**PF_6	**7**PF_6	**9**BF_4[8b]
$Cp_{C(9)–C(13)}$–$Cp_{C(19)–C(23)}$	22.3(2)	20.5(8)	19.7(6)	19.1(15)	17.5
$Cp_{C(9)–C(13)}$–naphthalene[a]	53.5(2)	45.6(6)	77.9(8)	45.6(12)	58.0
$Cp_{C(19)–C(23)}$–naphthalene[a]	53.0(2)	48.4(7)	60.5(8)	48.6(12)	60.8
C(19)–C(1)–C(8)–C(9)	23.3	31.3	28.9	29.4	25.2
C(1)–C(19)	148.0(5)	147(2)	148(2)	149(3)	148.4
C(8)–C(9)	148.3(5)	151(2)	150(2)	153(3)	148.9
C(1)–C(8)	255.6(5)	254(2)	257(2)	258(2)	254.1
C(9)–C(19)	291.4(5)	291(2)	288(1)	290(2)	286.9
Fe(1)–M	–	651.9	658.6	657.9	651.3
$Cent_{C(9)–C(13)}$–$Cent_{C(14)–C(18)}$[b]	330.5(3)	331.0(9)	330.8(8)	332(2)	329.6
$Cent_{C(19)–C(23)}$–$Cent_{C(24)–C(28)}$[b]	–	341(1)	362.5(8)	365(2)	343.5
$Cent_{C(9)–C(13)}$–$Cent_{C(19)–C(23)}$[b]	330.4(3)	323.1(9)	318.6(7)	319(2)	317.9

[a] Best plane of the adjacent six-membered naphthalene ring. [b] Cent: centroid of the corresponding Cp ligand.

does not cause tilt angles that deviate distinctly from those obtained for other comparable naphthalene derivatives,[8,18] which points out that the distortion is not a consequence of the steric hindrance between the positions C2 and C7, and the distal Cp ligands, but rather a result of the steric repulsion of the two-faced Cp units in the *peri* position (compare also data in Table 2). Despite the distortion of the entire *peri*-disubstituted naphthalene derivatives, a projection along the molecular axis of the sandwich complexes still shows an almost complete face-to-face arrangement of the sandwich units (Figure 7). This nicely demonstrates the clamp function of the naphthalene backbone for the purpose of stacking the sandwich units.

Spectroscopic Properties

The NMR signals of the complexes **3**, **5**, **6**PF_6, **7**PF_6 and **8**PF_6 have been assigned by means of ^1H, ^{13}C, $^1H^1H$ COSY, HMQC, ATP and $^1H^1H$ NOESY spectra. For comparison, the symmetrical diferrocenyl-substituted naphthalene congener **9**[8] was studied. The ^1H NMR signals of the sandwich units are found in the typical range for the corresponding unsubstituted derivatives. The deviations are difficult to explain, because they are small and probably strongly dominated by the anisotropy effects of the neighboring sandwich complex. The ^{13}C NMR shifts, which are less influenced by anisotropy effects compared to the overall shift range, illustrate a slight but distinct low-field shift for the signals of the unsubstituted Cp ligand as well as of the carbon nuclei in 2,5- and 3,4-positions of the naphthalene-bound Cp ligand of the ferrocenyl substituent in the order **5** < **9** < **3** < **8**PF_6 < **6**PF_6 < **7**PF_6. The order may reflect a subtle decrease of the electron repulsion between the ferrocenyl substituent and the neighboring sandwich complex (Table 3).

UV/Vis spectroscopy is a well-tried tool for obtaining initial information about potential nonlinear optical (NLO) behavior in virtue of the solvatochromism of dipolar com-

Table 3. NMR spectroscopic data of the ferrocenyl substituents in **3a**, **5**, **6**PF_6, **7**PF_6, **8**PF_6 and **9**.

	ML	$\delta(C_5H_5)$	δ(H-2′′,5′′)	δ(H-3′′,4′′)	$\delta(C_5H_5)$	δ(C-2′′,5′′)	δ(C-3′′,4′′)	δ(C-1′′)
3a	–	3.96	4.30	4.03	69.9	72.1/70.7	67.2/66,7	n.d.[a]
5	[FeCp*]	3.83	4.12	3.86	69.4	70.5	66.4	87.5
6PF_6	$[RhCp^*]^+$	3.98	4.31	4.10	70.5	72.2	68.3	92.5
7PF_6	$[IrCp^*]^+$	3.99	4.35	4.14	71.0	72.7	68.7	92.8
8PF_6	$[Ru(C_6H_6)]^+$	3.98	4.32	4.11	69.9	71.8	67.6	n.d.[a]
9	[FeCp]	3.86	4.11	3.84	69.5	70.9	66.5	91.3

[a] n.d.: not detectable.

Table 4. UV/Vis data of the complexes **3a**, **5**, **5**PF_6, **6**PF_6, **7**PF_6 and **8**PF_6.

		λ_{max}[a] (ε)[b] $\tilde{\nu}_{max}$[c]		λ_{max}[a] (ε)[b] $\tilde{\nu}_{max}$[c]	
	ML	MeOH	CH_2Cl_2	MeOH	CH_2Cl_2
3a	–	296 (6000)		458 (290)	456 (540)
		33784	[d]	21834	21930
5	[FeCp*]	296 (13000)		477 (1355)	481 (1930)
		33794	[d]	20964	20790
5PF_6	$[FeCp^*]^+$	304 (24780)		428 (3712, sh)[e]	433 (2850, sh)[e]
		32895	[d]	23364	23095
6PF_6	$[RhCp^*]^+$	293 (19170)			
		34130	[d]	[f]	[f]
7PF_6	$[IrCp^*]^+$	289 (5271)		450 (220)	454 (780)
		34602	[d]	22222	22026
8PF_6	$[Ru(C_6H_6)]^+$	286 (3758)		461 (190)	463 (960)
		34965	[d]	21602	21598

[a] In nm. [b] In $M^{-1}\cdot cm^{-1}$. [c] In cm^{-1}. [d] Beyond solvent range. [e] Shoulder. [f] Shoulder, not resolved.

pounds. If the dipole moments of the ground and an excited state are different, a variation of the solvent polarity will stabilize the two states differently, resulting in a bathochromic or hypsochromic shift of the absorption maximum.[19,20] Therefore, the UV/Vis spectra of the complexes **3**, **5**, **5**PF_6, **6**PF_6, **7**PF_6 and **8**PF_6 were recorded in dichloromethane and methanol (Table 4). For both solvents, weak absorption bands can be detected in the region at $\lambda \approx 300$ and 450 nm because of d–d transitions typical for ferrocenes.[21,22] The high-energy d–d transition is superimposed by a strong π–π* transition at $\lambda < 300$ nm, and is thus only observable as a shoulder. The dependence of the absorption maxima on the polarity of the solvent is minor: only a small hypsochromic shift is observed for the low-energy d–d transition. **5**PF_6 and **9**PF_6 demonstrate additional absorption bands at $\lambda_{max} = 813$ nm ($\varepsilon = 649\ M^{-1}cm^{-1}$) and at about 840 nm ($\varepsilon = 800\ M^{-1}cm^{-1}$),[8a] respectively, which are typical for ferrocenium derivatives, as well as very broad absorption bands at $\lambda_{max} = 1284$ nm ($\tilde{\nu} = 7788\ cm^{-1}$) and $\lambda_{max} = 1500$ nm[8a] ($\tilde{\nu} = 6667\ cm^{-1}$) ($\Delta\tilde{\nu}_{1/2} > 4000\ cm^{-1}$, $\varepsilon < 100\ M^{-1}cm^{-1}$, respectively. The NIR bands are indicative of mixed-valence charge-transfer (MVCT) transitions in mixed-valence compounds of class II.[9a,9b,23a,23b]

Redox Properties

Cyclic voltammograms were obtained for all of the naphthalene derivatives in this study. For comparison, the redox behavior of the 1,8-diferrocenyl-substituted naphthalene **9** was additionally investigated. As expected, all complexes reveal an electrochemically reversible one-electron oxidation in the range of ferrocene itself (Table 5, Figure 8), and can thus be assigned to the oxidation of the ferrocenyl substituent. The peak-to-peak separations found ($\Delta E_p = E_{pc} - E_{pa}$) are generally larger than the ideal value of 60 mV for a fully reversible one-electron process, which is probably due to the uncompensated solution resistance.

The cyclic voltammograms of the diiron complexes **5** and **9** contain an additional reversible one-electron redox wave due to the oxidation of the second ferrocenyl unit. The permethylation of one of the cyclopentadienyl ligands causes a more pronounced cathodic shift of the first oxidation step for **5** relative to **9**. The rhodium and ruthenium congeners display an irreversible reduction beyond –2000 mV vs. ferrocene/ferrocenium, which is caused by the reduction of the cationic sandwich unit;[24,25] for the iridium derivative **7**PF_6 a corresponding reduction was not observed within the accessible range, which seems reasonable, as the reduction potential for the cationic sandwich complex $[CpIr(C_5Me_5)]^+$ is about 500 mV more negatively shifted than for the corresponding rhodium complex.[25] A reduction of the aromatic π-system of the naphthalene unit is not expected within the scan range, because naphthalene reveals a reduction beyond –3 V vs. ferrocene/ferrocenium.[26]

When the oxidation potentials of the ferrocene units of all the monocationic species under study are compared, an increase is observed in the order **5**PF_6 < **3** < **7**PF_6 < **6**PF_6 < **8**PF_6 < **9**PF_6. It is still under discussion whether the

Table 5. Redox potentials[a] of the complexes **3a**, **5**PF_6, **6**PF_6, **7**PF_6, **8**PF_6 and **9**PF_6.

	ML	$E_{1/2}$ (1)[b]	ΔE_p (1)[c]	$E_{1/2}$ (2)[b]	ΔE_p (2)[c]	E_{pc}[d]	ΔE
3a	–	–0.036	0.102	–	–	–	–
5PF_6	$[FeCp^*]^+$	–0.042	0.097	–0.532	0.107	–	0.490[e]
6PF_6	$[RhCp^*]^+$	0.041	0.073	–	–	–2.157[d]	2.198[f]
7PF_6	$[IrCp^*]^+$	0.036	0.084	–	–	–	–
8PF_6	$[Ru(C_6H_6)]^+$	0.053	0.070	–	–	–2.345[d]	2.398[f]
9PF_6	$[FeCp]^+$	0.106	0.069	–0.098	0.84	–	0.204[e]

[a] In CH_2Cl_2 at room temperature, $[nBu_4N]PF_6$ (0.4 M) as supporting electrolyte, $Ag/AgPF_6$ as standard elektrode referenced vs. $E_{1/2}$(ferrocene/ferrocenium) = 0 V, scan rate 100 mV/s. [b] Potentials E ±0.005 V. [c] $\Delta E_p = |E_{pc} - E_{pa}|$. [d] Peak potential E_{pc} of the irreversible reduction. [e] $\Delta E = |E_{1/2}(1) - E_{1/2}(2)|$. [f] $\Delta E = |E_{1/2}(1) - E_{pc}|$.

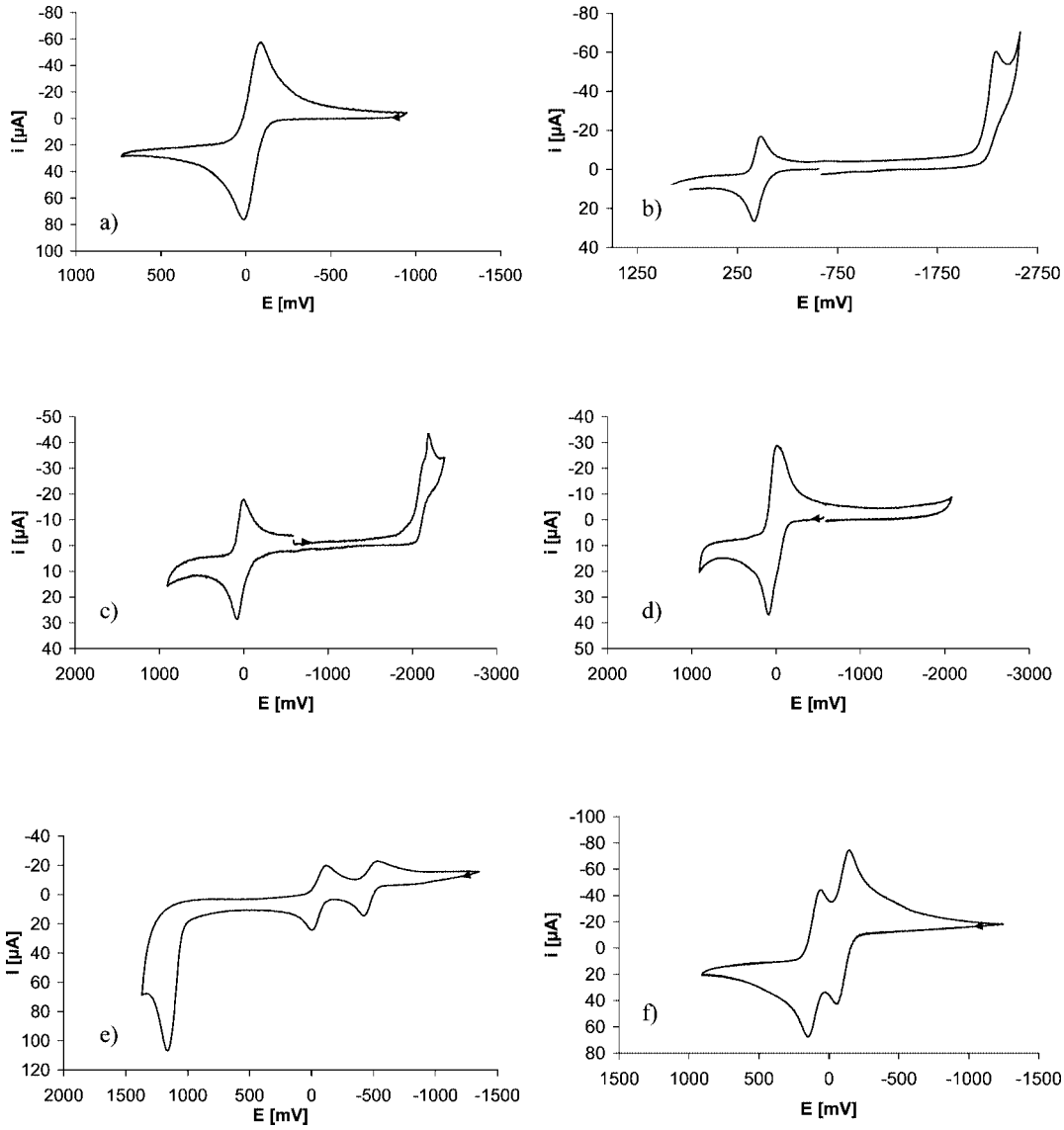

Figure 8. Cyclic voltammograms of **3** (a), **8**PF_6 (b), **6**PF_6 (c), **7**PF_6 (d), **5**PF_6 (e), **9** (f) (for more details see Table 5).

oxidation potentials are mainly influenced by a direct "through-space" interaction of the sandwich units, which are in an almost perfect face-to-face arrangement, or by a "through-bond" interaction facilitated by the π-bonding system of the naphthalene core. However, some arguments point to a predominant contribution of the "through-space" interaction: (i) the almost perpendicular conformation of the sandwich substituents with respect to the naphthalene plane hampers the interaction between the sandwich and naphthalene π-bonding systems and (ii) the 1,8-disubstitution of the aromatic naphthalene system disfavours the π-interaction between the substituents. This has been demonstrated by 1,3-diferrocenylated benzene derivatives, which may be regarded electronically similar to the 1,8-diferrocenylated naphthalene species; the benzene compounds reveal a difference in the oxidation potentials for the ferrocene units of less than 100 mV, although the ferrocene substituents rotate around the benzene–ferrocene σ-bond and can thus adopt a coplanar conformation of the ferrocene and benzene π-systems suitable for a proper π-interaction.[27,28] In contrast to this and in accordance with others,[8] a difference in the oxidation potentials of about 200 mV was found for **9**. The interpretation of an important "through-space" interaction in face-to-face stacked sandwich complexes is also in harmony with the explanation of an antiferromagnetic coupling between two paramagnetic trovacene complexes in *peri* position of naphthalene.[18]

Measurements Concerning Second Harmonic Generation

In order to elucidate the NLO activity of the stacked sandwich compounds with respect to second harmonic generation (SHG), hyper-Rayleigh scattering (HRS) measurements were performed for liquid solution samples of **5**PF_6,

6PF_6, **7**PF_6, **8**PF_6, and **9**PF_6 with a pulsed Nd:YAG laser at λ = 1064 and 1500 nm. The measurements were carried out as described in the literature.[29,30] Dichloromethane and acetonitrile were used as solvents. In addition, the Kurtz-powder method[31] was applied for crystalline samples of **5**PF_6, **6**PF_6 and **7**PF_6, because they crystallize in the chiral space group $C222_1$. However, no method could detect a measurable intensity of a frequency-doubled light. One explanation for the lack of SHG of the liquid solution samples is the weak polarizability and thus hyperpolarizability of the polar complexes, which can already be suggested from small solvatochromism. Even for the mixed-valence diferrocenyl species **5**PF_6 and **9**PF_6, which illustrate broad absorption bands in the NIR region (vide supra), no frequency-doubled signal could be detected, although SHG has been observed for species containing two ferrocene termini, which are separated by a cumulenium bridge.[32] The considerable absorption of **5**PF_6 and **9**PF_6 at $\lambda < 800$ nm may hamper the recognition of the second harmonic signal by absorption of light over a long range in the visible region. The lack of a SHG of the crystalline phase may be due to the orthorhombic crystal space group $C222_1$, which is a less effective space group for second harmonic generation.[33]

Conclusions

In order to create second harmonic generation by "through-space" hyperpolarization in two face-to-face, but polar arranged sandwich complexes, four novel disandwich complexes have been synthesized, wherein a ferrocene and a cationic sandwich complex are combined and held together by a naphthalene clamp. The synthesis was performed by two consecutively conducted cross-coupling reactions of cyclopentadienylzinc chloride and ferrocenylzinc chloride, respectively, with 1,8-diiodonaphthalene as starting material. After deprotonation of the free cyclopentadienyl substituent, the coordination of different half-sandwich units revealed the desired dinuclear complexes. In addition, the neutral, but unsymmetrical diferrocenyl derivative **5**, was oxidized to the monocationic dipolar compound **5**PF_6. For compounds **3**, **5**PF_6, **6**PF_6, **7**PF_6 the molecular structures have been determined by X-ray structure analysis. Complex **3** crystallizes in the space group $P2_1/c$, whereas the dinuclear species crystallize in the chiral space group $C222_1$. The fixation of the sandwich entities in the *peri* position of the naphthalene backbone causes severe distortion of the entire complex, but warrants an almost linear face-to-face alignment of the two sandwich units. The redox properties of all of these complexes turned out a "through-space" polar interaction, which influences the oxidation potential of the ferrocene unit in **5**PF_6, **6**PF_6, **7**PF_6 and **8**PF_6. However, no SHG effect could be detected by means of HRS measurements. Having in mind the chirality of the crystalline material of **5**PF_6, **6**PF_6 and **7**PF_6, the Kurtz-powder method has been applied, but again, no SHG effect could be observed. The lack of SHG in the stacked sandwich entities may raise some doubts about the applicability for SHG in stacked π-systems. To obtain a deeper insight into the "through-space" interaction concerning NLO effects it would be worthwhile to extend the amount of face-to-face stacked sandwich complexes in a polar fashion to make the π-electronic system more polarizable, which is subject of current work.

Experimental Section

General: Manipulations were carried out under dry nitrogen using standard Schlenk technique. Solvents were saturated with nitrogen. Diethyl ether (Et_2O), tetrahydrofuran (THF), *n*-hexane and toluene were freshly distilled from the appropriate alkali metal or metal alloy. Dichloromethane (CH_2Cl_2) and nitromethane ($MeNO_2$) were dried with calcium hydride. NMR: Varian Gemini 200 BB; Bruker AM 360; measured at 295 K rel. to TMS. UV/Vis: Perkin–Elmer Model 554. IR: KBr pellets; FT-IR Perkin–Elmer Model 325. MS: Finnigan MAT 311 A (EI-MS). Elemental analyses: CHN-O-Rapid, Fa. Heraeus, Zentrale Elementanalytik, Fachbereich Chemie, Universität Hamburg. 1,8-Diiodonaphthalene,[10] di-μ-chlorobis[chloro(η^5-pentamethylcyclopentadienyl)rhodium(III)] [Cp*$RhCl_2]_2$,[34] di-μ-chlorobis[chloro(η^5-pentamethylcyclopentadienyl)iridium(III)] [Cp*$IrCl_2]_2$,[34] di-μ-chlorobis[chloro(η^6-benzene)ruthenium(II)] $[(C_6H_6)RuCl_2]_2$,[35] ferrocenium hexafluorophosphate [FcH]PF_6,[36] chloro-(η^5-pentamethylcyclopentadienyl)-(tetramethylethylenediamine)iron(II) [Cp*Fe(tmeda)Cl][37] were synthesized according to literature procedures. Zinc chloride was dried by stirring in thionyl chloride unter reflux for several hours. $[Pd(PPh_3)_4]$ was purchased commercially.

1-Cyclopentadienyl-8-iodonaphthalene (2): The synthesis was carried out similar to the reaction described in the literature.[7c] Cyclopentadienyllithium (1.82 g, 25.25 mmol) and anhydrous zinc chloride (7.35 g, 53.95 mmol) were stirred in THF (70 mL) at 0 °C for 45 min. 1,8-Diiodonaphthalene (**1**) (4.97 g, 13.08 mmol) was added, the reaction mixture was warmed to room temperature and was stirred for 50 h. The reaction mixture was hydrolyzed with saturated NH_4Cl solution (150 mL), and the products were extracted with Et_2O (total amount 450 mL). The organic layer was dried with $MgSO_4$ and the solvents were evaporated to dryness. Extraction with hexane revealed 1-cyclopentadienyl-8-iodnaphthalene (**2**) as a yellow oil composed of three different isomers (3.55 g, 85.2%). M.p. ca. –10 °C. ^{1}H NMR (360 MHz, $CDCl_3$, rel. to TMS, room temp.): δ = 8.21 (dd, $^3J_{6,7}$ = 7.2, $^4J_{5,7}$ = 3.6 Hz, 1 H, 7-H), 7.86 (dd, $^3J_{5,6}$ = 7.2, $^4J_{5,7}$ = 3.6 Hz, 1 H, 5-H), 7.75–7.79 (m, 1 H, 3-H), 7.44 (d, $^3J_{2,3}$ = 5 Hz, 1 H, 2-H), 7.42 (d, $^3J_{3,4}$ = 5 Hz, 1 H, 4-H), 7.07 ("t", $^3J_{6,7}$ = $^3J_{5,6}$ = 7.2 Hz, 1 H), 6.62–6.70 (m, 3 H, Cp-H_{vinyl}), 3.12–3.14 (m, 1 H, sp^3-CpH) ppm. IR (KBr): $\tilde{\nu}$ = 3049, 2960, 2927, 2908, 2846, 1927, 1802, 1719, 1595, 1571, 1536, 1498 1437, 1419, 1362, 1352, 1321, 1250, 1221, 1194, 1175, 1139, 1106, 1037, 1001, 950, 928, 890, 860, 826; 815, 764, 726, 681, 641, 606, 581, 557, 522, 505, 466, 419 cm^{-1}.

Monolithioferrocene: Monolithioferrrocene was prepared similar to the procedure described in the literature.[11] A pentane solution of *t*BuLi (1.48 M, 35 mL, 51.63 mmol) was added dropwise to a solution of ferrocene (10.0 g, 5.37 mmol) in THF (25 mL) at room temperature. After 15 min of stirring, the solution was cooled to –15 °C. The addition of *n*-hexane led to the precipitation of the lithiated products, which contain the monolithiated ferrocene as the main product (3.50 g, 34%). The orange solid material is extremely oxygen- and moisture-sensitive.

1-Cyclopentadienyl-8-ferrocenylnaphthalene (3): Anhydrous zinc chloride (2.21 g, 16.2 mmol) was added to a solution of monolithioferrocene (2.317 g, 12,07 mmol) in THF (30 mL) at 0 °C. After stirring for 1 h, the red solution was added to a solution of 1-cyclopentadienyl-8-iodonaphthalene (**2**) (2.57 g, 8.08 mmol) and tetrakis(triphenylphosphane)palladium(0) (0.55 g, 0.48 mmol, 6 mol-%) in THF (10 mL). The reaction mixture was stirred at room temperature for 4 h and poured into a solution of saturated ammonium chloride (200 mL). The mixture was vigorously stirred and extracted with Et_2O. The orange-red organic layer was dried with $MgSO_4$. The volume of the solution was reduced to a minimum amount, dissolved in hexane/Et_2O (10:1), filtered through a column of alumina (5% water), and subjected to column chromatography on basic alumina [5% water, hexane/Et_2O (1:0 to 10:1)]. Unreacted ferrocene could be separated first. The second fraction contained the desired compound **3** as an orange-red solid material, consisting of two isomers: 1-(cyclopentadien-1′-yl)-8-(ferrocen-1′′-yl)naphthalene (**3a**) and 1-(cyclopentadien-2′-yl)-8-(ferrocen-1′′-yl)naphthalene (**3b**) (1.90 g, 63%). $C_{25}H_{20}Fe$ (376.28): calcd. C 79.80, H 5.36; found C 79.74, H 5.80. M.p. 122–125 °C; ref.[7c] 134–140 °C. ^{1}H NMR (200 MHz, $CDCl_3$, rel. to TMS, room temp.): δ = 8.18 (d, $^3J_{6,7}$ = 8 Hz, 1 H, 7-H), 7.79 (m, 2 H, H-2, 5-H), 7.50 (t, $^3J_{6,7}$ = $^3J_{5,6}$ = 7.5 Hz, 1 H, 6-H), 7.32–7.42 (m, 2 H, H-3, 4-H), 5.88–6.30 (m, 3 H, Cp-H_{vinyl}), 4.30, 4.26 (br. t, 2 H, Fc-$H_{2,5}$, isomer **3a** and **3b**), 4.03 (br. t, Fc-$H_{3,4}$, 1.2 H, isomer **3b**), 3.96 (br. s, 5.8 H, Fc-H, isomer **3a** and **3b**, Fc-$H_{3,4}$ isomer **3a**), 2.89 (br. s, 0.6 H, sp^3-CpH, isomer **3b**), 2.68 (br. s, 0.4 H, sp^3-CpH, isomer **3a**) ppm. ^{13}C NMR (50 MHz, $CDCl_3$, rel. to TMS, room temp.): δ = 137.4, 136.3 (C-1, C-8); 133.2, 132.6, 132.1, 131.9, 129.5, 129.5, 129.20, 128.7, 128.2, 127.8, 125.5, 125.1, 72.1, 70.7 (C-2′′,5′′); 69.9 (C_5H_5), 67.2, 66.7 (C-3′′,4′′), 44.7, 41.7 (sp^{3}C-C_5H_5) ppm. IR (KBr): $\tilde{\nu}$ = 3076, 3046, 2916, 2897, 2871, 1637, 1591, 1570, 1500, 1478, 1422, 1365, 1105, 1052, 1032, 1022, 999, 952, 894, 824, 810, 773, 673, 485 cm^{-1}. MS (EI): *m/z* (%) = 376.3 (100) [M$^+$], 310.3 (59) [M – C_5H_6]$^+$, 254 (23) [$C_{10}H_6(C_5H_4)_2^+$], 189 (16) [$C_{10}H_5(C_5H_4)^+$], 121 (16) [FeCp$^+$]. UV/Vis (CH_2Cl_2): λ_{max} (ε) = 382 (1420, sh), 456 (536 M^{-1}cm^{-1}) nm; (MeOH): λ_{max} (ε) = 295 (ca. 6000), 378 (ca. 800), 458 (ca. 300 M^{-1}cm^{-1}) nm.

1-[(η^5-Cyclopentadienediyl)(η^5-pentamethylcyclopentadienyl)iron(II)]-8-ferrocenylnaphthalene (5): 1-Cyclopentadienyl-8-ferrocenylnaphthalene (**3**) (0.182 g, 0.48 mmol) was dissolved in THF (10 mL), treated with an Na[N($SiMe_3$)$_2$] solution in THF (1 M, 0.5 mL, 0.5 mmol) at 0 °C and stirred for 90 min. To this solution, which was cooled to –78 °C, [Cp*Fe(tmeda)Cl] (0.412 g, 1.2 mmol) was added. After stirring overnight and warming to room temperature, the reaction mixture was concentrated to dryness. The residue was dissolved in a minimum amount of toluene and filtered through alumina (neutral, 5% water) and the filtrate was purified by column chromatography on alumina (neutral, 5% water). As eluent *n*-hexane/toluene (10:1) was used. The eluate was concentrated to dryness, to yield 1-[(η^5-cyclopentadienediyl)(η^5-pentamethylcyclopentadienyl)iron(II)]-8-ferrocenylnaphthalene (**5**) (0.18 g, 65%) as an orange crystalline material (Figure 9). $C_{35}H_{34}Fe_2$ (566.35): calcd. C 74.23, H 6.05; found C 73.99, H 6.59. M.p. 150 °C. ^{1}H NMR (200 MHz, $CDCl_3$ rel. to TMS, room temp.): δ = 8.06 (dd, $^3J_{6,7}$ = 7.5, $^4J_{5,7}$ = 2 Hz, 1 H, 7-H), 7.93 (d, $^3J_{2,3}$ = 6.5 Hz, 1 H, 2-H), 7.74 (dt, 2 H, H-4, 5-H), 7.48 (t, $^3J_{6,7}$ = $^3J_{5,6}$ = 7.5 Hz, 1 H, 6-H), 7.45 (t, $^3J_{3,4}$ = $^3J_{2,3}$ = 6.5 Hz, 1 H, 3-H), 4.12 (t, ^3J = 2 Hz, 2 H, 2′′,5′′-H), 3.86 (t, ^3J = 2 Hz, 2 H, 3′′,4′′-H), 3.83 (s, 5 H, C_5H_5), 3.64 (t, ^3J = 2 Hz, 2 H, 2′,5′-H), 3.38 (t, ^3J = 2 Hz, 2 H, 3′,4′-H), 1.60 (s, 15 H, C_5Me_5) ppm. ^{13}C NMR (50 MHz, $CDCl_3$ rel. to TMS, room temp.): δ = 136.9 (C-8), 135.3 (C-1), 131.2 (C-7), 130.5 (C-2), 126.6, 126.1 (C-4,5), 124.2 (C-6), 124.0 (C-3), 91.2 (C-1′), 87.5 (C-1′′), 79.7 (C_5Me_5), 72.8 (C-2′,5′), 71.5 (C-3′,4′), 70.5 (C-2′′,5′′), 69.4 (C_5H_5), 66,40 (C-3′′,4′′), 10,81 (C_5Me_5) ppm. IR (KBr):$\tilde{\nu}$ = 3089, 3054, 2943, 2900, 2853, 1636, 1571, 1506, 1476, 1448, 1425, 1414, 1377, 1365, 1314, 1266, 1182, 1137, 1105, 1066, 1032, 999, 935, 912, 881, 843, 825, 811, 788, 772, 692, 661, 640, 602, 587, 533, 521, 510, 494, 483, 460, 432, 423, 414, 408 cm^{-1}. MS (EI): *m/z* (%) = 566 (100) [M$^+$], 501 (24) [M – Cp]$^+$, 431 (12) [M – Cp*]$^+$, 445 (6) [M – Cp]$^+$, 375 (3) [M – FeCp*]$^+$, 310 (46) [M – CpFeCp*]$^+$, 254 (6) [$C_{10}H_6(C_5H_4)_2$]$^+$, 189 (6) [$C_{10}H_5(C_5H_4)$]$^+$, 121 (5) [FeCp]$^+$. UV/Vis (CH_2Cl_2): λ_{max} (ε) = 298 (18240), 391 (2390, sh), 481 (1932 M^{-1}cm^{-1}) nm; (MeOH): λ_{max} (ε) = 296 (ca. 13000), 398 (ca. 1600, sh), 477 (ca. 1355 M^{-1}cm^{-1}) nm.

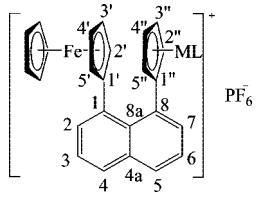

Figure 9. Numbering scheme for the assignment of the NMR signals.

1-[(η^5-Cyclopentadienediyl)(η^5-pentamethylcyclopentadienyl)iron(III)]-8-ferrocenylnaphthalene Hexafluorophosphate (5PF$_6$): 1-[(η^5-Cyclopentadienediyl)(η^5-pentamethylcyclopentadienyl)iron(II)]-8-ferrocenylnaphthalene (**5**) (0.314 g, 0.55 mmol) was dissolved in CH_2Cl_2 (30 mL). Ferrocenium hexafluorophosphate (0.166 g, 0.50 mmol) was added, whereupon the color of the reaction mixture changed form orange-red to dark brown. After stirring at room temperature for 80 min, *n*-hexane (60 mL) was layered on the CH_2Cl_2 solution, and the reaction flask was stored at –30 °C for 2 d. The precipitated crystals were filtered off and dried in vacuo. 1-[(η^5-Cyclopentadienediyl)(η^5-pentamethylcyclopentadienyl)iron(III)]-8-ferrocenylnaphthalene hexafluorophosphate (**5**PF$_6$) was obtained in dark red-brown crystals (0.32 g, 0.45 mmol, 82%). $C_{35}H_{34}Fe_2PF_6{\cdot}(CH_2Cl_2)_{0.66}$ (767.94): calcd. C 55.78, H 4.64; found C 55.98, H 4.70. M.p. 189 °C (dec). ^{1}H NMR (360 MHz, [D$_6$]acetone, rel. to TMS, room temp.): δ = 34.2 (2′,5′-H), 24.9 (2′′,5′′-H), 22.5 (3′′,4′′H), 18.5 (3′,4′-H), 10.9 (C_5H_5), 1.87 (4-H, 5-H), –2.22 (6-H), –10.81 (7-H), –25.26 (3-H), –36.55 (C_5Me_5), –55.84 (2-H). IR (KBr): $\tilde{\nu}$ = 3121, 3051, 2963, 2916, 1631, 1587, 1502, 1474, 1448, 1423, 1412, 1389, 1314, 1268, 1185, 1133, 1105, 1070, 1032, 1000, 935, 919, 846, 837, 775, 732, 699, 692, 638, 598, 557, 533, 521, 510, 494, 483, 460, 432, 423, 414, 408 cm^{-1}. MS (FAB): *m/z* (%) = 566 (100) [M$^+$], 501 (8) [M – Cp]$^+$, 445 (12) [M – FeCp]$^+$, 431 (20) [M – Cp*]$^+$, 310 (44) [M – CpFeCp*]$^+$. UV/Vis (CH_2Cl_2): λ_{max} (ε) = 433 (2850, sh), 813 (649), 1284 (122 M^{-1}cm^{-1}) nm; MeOH: λ_{max} (ε) = 304 (24780), 428 (3712, sh), 801 (953 M^{-1}cm^{-1}) nm.

1-[(η^5-Cyclopentadienediyl)(η^5-pentamethylcyclopentadienyl)-rhodium(III)]-8-ferrocenylnaphthalene Hexafluorophosphate (6PF$_6$): 1-Cyclopentadienyl-8-ferrocenylnaphthalene (**3**) (0.29 g, 0.77 mmol) was dissolved in THF (15 mL), and treated with a solution of Na[N($SiMe_3$)$_2$] in THF (1 M, 0.75 mL, 0.75 mmol) at 0 °C. After stirring for 80 min, the solvent was stripped off in vacuo, and the residue was redissolved in acetonitrile (50 mL), whereupon thallium(I) chloride (0.185 g, 0,77 mmol) was added. The reaction mixture was stirred at room temperature for 3 h and at 40 °C for 18 h. [Cp*RhCl$_2$]$_2$ (0.236 g, 0.38 mmol) was added and the mixture stirred at 45 °C for 3 h and at room temperature for 20 h. The reaction solution was filtered through Celite, and the filtrate was concentrated to dryness. The solid red residue was dissolved in water (60 mL) and, after filtration, NH_4PF_6 (0.150 g, 1.03 mmol), dis-

solved in water (5 mL), was added to the filtrate. An orange, voluminous precipitate formed, which was collected on a filter frit, washed with water and Et_2O and dried in vacuo. For recrystallization the orange-red powder of **6**PF_6 (0.425 g, 0.57 mmol, 74%) was redissolved in CH_2Cl_2 and overlayered with Et_2O. $C_{35}H_{34}FeRhPF_6$ (758.37): calcd. C 55.43, H 4.52; found C 56.48, H 4.87. M.p. 172 °C (dec). ^{1}H NMR (200 MHz, [D$_6$]acetone, rel. to TMS, room temp.): δ = 8.33 (dd, $^3J_{2,3}$ = 7.5, $^4J_{2,4}$ = 1,5 Hz, 1 H, 2-H), 8.03 (dd, $^3J_{6,7}$ = 8, $^4J_{5,7}$ = 2 Hz, 1 H, 7-H), 7.94 (dd, $^3J_{3,4}$ = 8, $^4J_{2,4}$ = 1.5 Hz, 1 H, 4-H), 7.74–7.61 (m, 3 H, 3-H, 5-H, 6-H), 5.62 (t, 2 H, ^3J = 2 Hz, 2′,5′-H), 5.38 (t, ^3J = 2 Hz, 2 H, 3′,4′-H), 4.31 (t, ^3J = 2 Hz, 2 H, 2′′,5′′-H), 4.10 (t, ^3J = 2 Hz, 2 H, 3′,4′-H), 3.98 (s, 5 H, C_5H_5), 1.94 (s, 15 H, C_5Me_5) ppm. ^{13}C NMR (50 MHz, [D$_6$]acetone, rel. to TMS, room temp.): δ = 136.4 (C-1), 135.9 (C-8), 133.7 (C-2), 131.9 (C-8a), 130.8 (C-7), 128.2 (C-4), 128.0 (C-4a), 126.3, 125.5 (C-5,6), 113.7 (C-1′), 101.6 [d, $^1J(^{13}C^{103}Rh)$ = 8 Hz, C_5Me_5], 92.5 (C-1′′), 88.4 [d, $^1J(^{13}C^{103}Rh)$ = 6 Hz C-2′, 5′], 87.7 [d, $^1J(^{13}C^{103}Rh)$ = 7.5 Hz, C-3′,4′], 72.2 (C-2′′,5′′), 70.5 (C_5H_5), 68.3 (C-3′′,4′′), 10.1 (C_5Me_5) ppm. IR (KBr): $\tilde{\nu}$ = 3093, 2919, 1626, 1500, 1476, 1455, 1425, 1389, 1314, 1266, 1185, 1133, 1106, 1068, 1028, 1001, 841, 773, 740, 692, 558, 481 cm^{-1}. MS (FAB): *m*/*z* (%) = 613 (100) [M$^+$], 548 (10) [M – Cp]$^+$,492 (13) [M – FeCp]$^+$,478 (18) [M – Cp*]$^+$, 375 (22) [M – RhCp*]$^+$, 357 (47) [M – Cp*-FeCp]$^+$. UV/Vis (MeOH): λ_{max} (ε) = 293 (19170 M^{-1} cm^{-1}) nm.

1-[(η^5-Cyclopentadienediyl)(η^5-pentamethylcyclopentadienyl)-iridium(III)]-8-ferrocenylnaphthalene Hexafluorophosphate (7PF_6): The synthesis of **7**PF_6 was carried out in the same manner as for **6**PF_6 with additional washing of the precipitate with toluene and hexane. Used quantities: 1-cyclopentadienyl-8-ferrocenylnaphthalene (**3**) (0.27 g, 0.72 mmol), THF (15 mL), Na[N(SiMe$_3$)$_2$] in THF (1 M, 0.72 mL, 0.72 mmol), thallium(I) chloride (0.225 g, 0.94 mmol), [Cp*IrCl$_2$]$_2$ (0.28 g, 0.35 mmol), water (60 mL), solution of NH_4PF_6 (0.150 g, 1.03 mmol) in water (5 mL). Yield: 0.373 g (61%) of orange-red powder of **6**PF_6, prior to recrystallization from CH_2Cl_2/Et_2O. $C_{35}H_{34}FeIrPF_6$·($C_6H_5CH_3$) (939.83): calcd. C 53.68, H 4.50; found C 54.11, H 4.58. M.p. 167 °C (dec). ^{1}H NMR (200 MHz, [D$_6$]acetone, rel. to TMS, room temp.): δ = 8.34 (dd, $^3J_{2,3}$ = 7, $^4J_{2,4}$ = 2 Hz, 1 H, 2-H), 8.00 (dd, $^3J_{6,7}$ = 7, $^4J_{5,7}$ = 2 Hz, 1 H, 7-H), 7.93 (dd, $^3J_{3,4}$ = 7, $^4J_{2,4}$ = 2 Hz, 1 H, 4-H), 7.69 –7.60 (m, 3 H, H-3, 5-H, 6-H), 5.70 (t, 2 H, ^3J = 2 Hz, 2′,5′-H), 5.37 (t, 2 H, ^3J = 2 Hz, 3′,4′-H), 4.35 (t, ^3J = 2 Hz, 2 H, 2′′,5′′-H), 4.14 (t, ^3J = 2 Hz, 2 H, 3′′,4′′-H), 3.99 (s, 5 H, C_5H_5), 2.02 (s, 15 H, C_5Me_5) ppm. ^{13}C NMR (50 MHz, [D$_6$]aceton/TMS, room temp.): δ = 137.0 (C-1), 136.6 (C-8), 134.5 (C-2), 133.5 (C-3), 132.6 (C-8a), 131.5 (C-7), 128.9 (C-4), 128.3 (C-4a), 126.9 (C-5), 126.2 (C-6), 107.8 (C-1′), 95.6 (C_5Me_5), 92.8 (C-1′′), 82.4 (C-2′,5′), 80.9 (C-3′,4′), 72.7 (C-2′′,5′′), 71.0 (C_5H_5), 68.7 (C-3′′,4′′), 10.0 (C_5Me_5) ppm. IR (KBr): $\tilde{\nu}$ = 3093, 2917, 1626, 1475, 1389, 1314, 1264, 1184, 1106, 1035, 1002, 843, 773, 692, 558, 483 cm^{-1}. MS (EI): *m*/*z* (%) = 703 (100) [M$^+$], 581 (14) [M – CpFe]$^+$, 568 (8) [M – Cp*]$^+$, 447 (15) [M – Cp* – FeCp]$^+$, 376 (52) [M – Cp*Ir]$^+$. UV/Vis (CH_2Cl_2): λ_{max} (ε) = 454 (780 M^{-1} cm^{-1}) nm; (MeOH): λ_{max} (ε) = 289 (5271), 450 (220 M^{-1} cm^{-1}) nm.

1-[(η^6-Benzene)(η^5-cyclopentadienediyl)ruthenium(II)]-8-ferrocenylnaphthalene Hexafluorophosphate (8PF_6): The synthesis of **8**PF_6 was carried out in the same mannere as for **6**PF_6 with additional washing of the precipitate with toluene and hexane. Used quantities: 1-cyclopentadienyl-8-ferrocenylnaphthalene (**3**) (0.33 g, 0.86 mmol), THF (20 mL), Na[N(SiMe$_3$)$_2$] in THF (1 M, 0.85 mL, 0.85 mmol), MeCN (50 mL), thallium(I) chloride (0.208 g, 0.87 mmol), [$C_6H_6RuCl_2$]$_2$ (0.205 g, 0.41 mmol), water (60 mL), solution of NH_4PF_6 (0,18 g, 1.07 mmol) in water (5 mL). Yield: 0.22 g (37%) of orange-red powder of **8**PF_6. $C_{31}H_{25}FeRuPF_6$·($C_6H_5CH_3$)$_{0.66}$ (760.85): calcd. C 56.30, H 4.02; found C 57.00, H 4.07. M.p. 318 °C (dec.). ^{1}H NMR (200 MHz, [D$_6$]acetone, rel. to TMS, room temp.): δ = 8.33 (dd, $^3J_{2,3}$ = 7.5, $^4J_{2,4}$ = 1.5 Hz, 1 H, 2-H), 7.99–7.90 (m, 3 H, 4-H, 5-H, 7-H), 7.62 (t, $^3J_{3,4}$ = 7.5 Hz, 1 H, 3-H), 7.50 (t, $^3J_{6,7}$ = $^3J_{5,6}$ = 7.5 Hz, 1 H, 6-H), 6.13 (s, 6 H, C_6H_6), 5.49 (t, ^3J = 2 Hz, 2 H, 2′,5′-H), 5.18 (t, ^3J = 2 Hz, 2 H, 3′,4′-H), 4.32 (t, ^3J = 2 Hz, 2 H, 2′′,5′′-H), 4.11 (t, ^3J = 2 Hz, 2 H, 3′′,4′′-H), 3.98 (s, 5 H, C_5H_5) ppm. ^{13}C NMR (50 MHz, [D$_6$]acetone, rel. to TMS, room temp.): δ = 133.6 (C-2), 133.5 (C-7), 130.3 (C-4), 129.0 (C-4a or 8a), 127.9 (C-5), 125.8 (C-3), 125.0 (C-6), 87.3 (C_6H_6), 82.0 (C-2′,5′), 78.4 (C-3′,4′), 71.8 (C-2′′,5′′), 69.9 (C_5H_5), 67.6 (C-3′′,4′′) ppm. IR (KBr): $\tilde{\nu}$ = 3090, 1629, 1509, 1480, 1441, 1395, 1365, 1187, 1146, 1106, 1067, 1028, 1002, 879, 841, 775, 739, 691, 558, 510, 484 cm^{-1}. MS (EI): *m*/*z* (%) = 555 (65) [M$^+$], 490 (5) [M – Cp]$^+$, 477 (15) [M – C_6H_6]$^+$, 376 (16) [M – C_6H_6Ru]$^+$, 311 (18) [M – C_6H_6RuCp]$^+$. UV/Vis (CH_2Cl_2): λ_{max} (ε) = 463 (960 M^{-1} cm^{-1}) nm; (MeOH): λ_{max} (ε) = 286 (3758), 461 (190 M^{-1} cm^{-1}) nm.

Cyclic Voltammetry: Measurements were performed in CH_2Cl_2 with 0.4 M [*n*Bu_4N]PF_6 as supporting electrolyte. An Amel 5000 system was used with a Pt wire as working electrode and a Pt plate (0.6 cm^2) as auxiliary electrode. The potentials were measured against Ag/$AgPF_6$ and were referenced to $E_{1/2}$(ferrocene/ferrocenium) = 0 V.

X-ray Structure Determination: Crystals of compound **3**, **5**PF_6, **6**PF_6 and **7**PF_6 suitable for an X-ray structure determination were obtained for compound **3** by careful evaporation of the solvent, and for **5**PF_6, **6**PF_6 and **7**PF_6 by slow diffusion of Et_2O into a CH_2Cl_2 solution of the complexes at –30 °C. The data were collected with a four-circle diffractometer by Hilger and Watts, Mo-K_α, λ = 0.71073 Å (Table 6). The structures were solved by direct methods (SHELXS-86)[38a] and the refinements on F^2 were carried out by full-matrix least-squares techniques (SHELXL-97).[38b] All non-hydrogen atoms were refined with anisotropic thermal parameters. The hydrogen atoms were refined with a fixed isotropic thermal parameter related by a factor of 1.2 to the value of the equivalent isotropic parameter of their carrier atoms. Weights were optimized in the final refinement cycles. Residual electron density was observed for crystals of **5**PF_6, **6**PF_6, and **7**PF_6 pointing out diffuse incorporation of solvent molecules.[39] CCDC-279705 (**3**), -279702 (**5**PF_6), -279703 (**6**PF_6), and -279704 (**7**PF_6) contain the supplementary crystallographic data for this paper. These data can be obtained free of charge from The Cambridge Crystallographic Data Centre via www.ccdc.cam.ac.uk/data_request/cif.

SHG Measurements: The efficiency of SHG of the crystalline materials are measured with our experimental setup[40] for the Kurtz powder method.[31] The measurements were performed at 1064 nm laser pulses produced by the Nd:YAG laser at low power (50 mJ per pulse); this laser produces 40-ns pulses with a repetition rate of 10 Hz. The procedure for the measurements is as follows: for crystalline samples, the grain size was not standardized. For this reason signals between individual measurements were seen to vary in some cases by as much as ±20%. The material to be measured was ground to a fine powder and compacted in a mount and installed in the sample holder. In order to compare the new samples with the reference urea, the measurements were averaged over several laser cycles. The voltage from the photomultiplier was measured by an oscilloscope which was triggered by the signal itself. The photomultiplier voltage and the neutral density filter area were optimized to obtain a good signal-to-noise ratio and to prevent the saturation of the photomultiplier. The oscilloscope measures the

Table 6. Crystallographic data of **3a**, **5**PF_6, **6**PF_6 und **7**PF_6.

	3a	**5**PF_6	**6**PF_6	**7**PF_6
Empirical formula	$C_{25}H_{20}Fe$	$C_{35}H_{34}Fe_2PF_6$	$C_{35}H_{34}FeRhPF_6$	$C_{35}H_{34}FeIrPF_6$
M_r [g/mol]	376.25	711.29	758.35	847.64
T [K]	153(2)	153(2)	153(2)	153(2)
λ [pm]	71.073	71.073	71.073	71.073
Crystal system	monoclinic	orthorhombic	orthorhombic	orthorhombic
Space group	$P2_1/c$	$C222_1$	$C222_1$	$C222_1$
a [pm]	1142.3(7)	1239.8(3)	1231.3(11)	1234.1(8)
b [pm]	985.1(6)	2377.0(5)	2408.3(18)	2405.1(9)
c [pm]	1903.2(10)	2271.4(5)	2277.8(18)	2279.0(18)
β [°]	123.71(4)			
V [10^6 pm^3]	1781.5(18)	6694(3)	6754.1(9)	6764(7)
Z	4	8	8	8
$\rho_{calcd.}$ [Mg/m^3]	1.403	1.412	1.492	1.665
μ [mm^{-1}]	0.851	0.971	1.021	4.463
F(000)	784	2920	3072	3328
Crystal size [mm]	0.50×0.50×0.20	0.30×0.40×0.50	0.80×0.15×0.10	0.50×0.20×0.50
$\theta_{min,max}$	2.26–27.45	2.48–25.08	2.46–27.56	2.46–25.06
Index range	$-5 \le h \le 14$	$-1 \le h \le 14$	$-16 \le h \le 1$	$-7 \le h \le 14$
	$-12 \le k \le 2$	$-1 \le k \le 28$	$-1 \le k \le 31$	$-9 \le k \le 28$
	$-24 \le l \le 22$	$-1 \le k \le 26$	$-1 \le l \le 29$	$-27 \le l \le 2$
Reflections total	6429	4059	5115	3421
Reflections independent	4068	3809	4827	3314
R_{int}	0.0342	0.0424	0.0349	0.0498
Reflections [$I > 4\sigma(I)$]	3022	1996	3880	2431
Parameters	253	436	437	402
GOF[a]	1.033	0.846	1.086	1.029
R_1/wR_2[b] [$I > 2\sigma(I)$]	0.0503/0.1158	0.0745/0.1548	0.0641/0.1733	0.0612/0.1371
R_1/wR_2[b] (all data)	0.0802/0.1307	0.1464/0.1842	0.0834/0.1891	0.0963/0.1534
Min./max. residue [e·Å^3]	–0.523/0.736	–0.398/0.905	–0.913/1.684	–1.681/1.564

[a] GOF = "Goodness-of-fit" = $\{\Sigma[w(F_o^2 - F_c^2)^2]/(n-p)\}^{1/2}$ (n = number of reflections, p = number of parameters). [b] $R_1 = \Sigma||F_o| - |F_c||$; $wR_2 = \{\Sigma[w(F_o^2 - F_c^2)^2]/\Sigma[w(F_o^2)]\}^{1/2}$.

time integral of the photomultiplier voltage automatically, which is proportional to the SHG efficiency. The oscilloscope also performs the average over several shots automatically. The SHG efficiency measurement for the reference sample was performed under the same experimental conditions as that of the test samples. The SHG efficiency for liquid solutions of the polar compounds was determined by means of hyper-Rayleigh scattering (HRS).[41] The HRS measurements were performed with a pulsed Nd:YAG laser at a wavelength of λ = 1064 and 1500 nm. For the experimental setup for HRS_{1064nm}, see ref.[28] Solutions of the complexes in dichloromethane and acetonitrile with concentrations in the range of 10^{-4} to 10^{-6} M were used with *p*-nitroaniline as a reference [$\beta(CH_2Cl_2)_{1064} = 21.6 \cdot 10^{-30}$ esu; $\beta(MeCN)_{1064} = 29.2 \cdot 10^{-30}$ esu].[42] The measurements at 1500 nm wavelength were carried out similar to the setup described in ref.[43] Instead of the third harmonic (355 nm), generated from an Nd:YAG laser with a wavelenghth of 1064 nm, the optical parametric oscillator (OPO)[44] in use was pumped with the second harmonic (532 nm). The signal intensity at 824 nm and the fundamental at 532 nm were removed from the idler by using dichroic mirrors (HR 650–850 and HR 532), a green light and a silicon filter (transparent > 1000 nm). An additional Glan–Taylor polarizer ensured the vertical polarization of the beam into the measurement cell. Measurements were performed with ca. 10^{-4}–10^{-6} M solutions of **5**, **7** and **8** in CH_2Cl_2. Disperse Red 1 (DR1) was used as an external standard with a value of β_{1500} (DR1) = $70 \cdot 10^{-30}$ esu. This value was obtained by comparing the slopes of the reference in CH_2Cl_2 and $CHCl_3$ to obtain the ratio of β_{solute}.[45] With the value $\beta(CHCl_3) = 80 \cdot 10^{-30}$ esu[46] the hyperpolarisibility of DR1 in CH_2Cl_2 is estimated to be $70 \cdot 10^{-30}$ esu. The effect of the refractive indices of the solvents was corrected using the simple Lorentz local field.[47]

Acknowledgments

This work was supported by the Deutsche Forschungsgemeinschaft (DFG, HE 1309/3), by the DAAD (Deutsch-Portugiesicher Wissenschaftleraustausch INIDA) and by the European Community (COST D14, TMR FMRX-CT98-0166). We thank the DEGUSSA AG for a donation of $RuCl_3$, the Sartorius GmbH for a donation of microfilters, and Nelson Lopes, GoLP, Centro de Física de Plasmas, Instituto Superior Técnico, Lisboa, Portugal, for performing the Kurtz powder measurements. M. H. G. thanks for financial support by Fundação para a Ciência e Tecnologia, project POCTI/QUI/48443/2002.

[1] F. Salhi, D. M. Collard, *Adv. Mater.* **2003**, *15*, 81–85.
[2] J. Cornil, D. Beljonne, J.-P. Calbert, J.-L. Brédas, *Adv. Mater.* **2001**, *13*, 1053–1067.
[3] J. S. Miller, A. J. Epstein, W. M. Reiff, *Acc. Chem. Res.* **1988**, *21*, 114–120; H. Atzkern, P. Bergerat, H. Beruda, M. Fritz, J. Hiermeier, P. Hudeczek, O. Kahn, F. H. Köhler, M. Paul, B. Weber, *J. Am. Chem. Soc.* **1995**, *117*, 997–1011.
[4] S. Di Bella, M. A. Ratner, T. J. Marks, *J. Am. Chem. Soc.* **1992**, *114*, 5842–5849; S. Di Bella, I. L. Fragalá, M. A. Ratner, T. J. Marks, *J. Am. Chem. Soc.* **1993**, *115*, 682–686.
[5] a) J. Zyss, I. Ledoux, S. Volkov, V. Chernyak, S. Mukamel, G. P. Bartholomew, G. C. Bazan, *J. Am. Chem. Soc.* **2000**, *122*, 11956–11962; G. P. Bartholomew, S. Ledoux, S. Mukamel, G. C. Bazan, J. Zyss, *J. Am. Chem. Soc.* **2002**, *124*, 13480–13485; b) A. Bahl, W. Grahn, S. Stadler, F. Feiner, G. Bourhill, C. Bräuchle, A. Reisner, P. G. Jones, *Angew. Chem.* **1995**, *107*, 1587–1590; W. Grahn, A. Bahl, S. Link, S. Stadler, R. Dietrich, K. Meerholz, C. Bräuchle, *Proc. SPIE – Int. Soc. Opt. Eng.*

1997, *3147*, 62–73; A. Bahl, PhD Thesis, Technical University of Braunschweig, **1997**.

[6] I. Ledoux, J. Zyss, A. Jutand, C. Amatore, *Chem. Phys.* **1991**, *150*, 117–123.

[7] a) M. Rosenblum, H. M. Nugent, K. D. Jang, M. M. Labes, W. Cahalane, P. Klemarczyk, W. M. Reiff, *Macromolecules* **1995**, *28*, 6330–6342; b) D. A. R. Hudson, B. M. Foxman, M. Rosenblum, *Organometallics* **1999**, *18*, 4098–4106; c) D. A. R. Hudson, B. M. Foxman, M. Rosenblum, *Organometallics* **2000**, *19*, 469–474.

[8] a) M.-L. Lee, B. M. Foxman, M. Rosenblum, *Organometallics* **1985**, *4*, 539–547; b) R. Arnold, B. M. Foxmann, M. Rosenblum, W. B. Euler, *Organometallis* **1988**, *7*, 1253–1259.

[9] a) M. Malessa, PhD Thesis, University of Hamburg, **2001**; b) M. Malessa, J. Heck, manuscript in preparation.

[10] H. O. House, D. G. Koepsell, W. J. Campbell, *J. Org. Chem.* **1972**, *37*, 1003–1011.

[11] a) F. Rebierre, O. Samuel, H. B. Kagan, *Tetrahedron Lett.* **1990**, *31*, 3121–3124; b) U. T. Müller-Westerhoff, Z. Yang, G. Ingram, *J. Organomet. Chem.* **1993**, *463*, 163–167; c) D. Guillaneux, H. B. Kagan, *J. Org. Chem.* **1995**, *60*, 2502–2505; R. Sanders, U. T. Mueller-Westerhoff, *J. Organomet. Chem.* **1996**, *512*, 219–224.

[12] W.-Y. Wong, W.-T. Wong, *J. Chem. Soc., Dalton Trans.* **1996**, 3209–3214.

[13] G. E. Herberich, C. Engelke, W. Pahlmann, *Chem. Ber.* **1979**, *112*, 607–624.

[14] J. D. Dunitz, *Acta Crystallogr., Sect. B* **1979**, *35*, 1068–1074.

[15] J. S. Miller, J. C. Calabrese, H. Rommelmann, S. Chittipeddi, J. H. Zhang, W. M. Reiff, A. J. Epstein, *J. Am. Chem. Soc.* **1987**, *109*, 769–781.

[16] S. Rittinger, D. Buchholz, M.-H. Delville-Desbois, J. Linares, F. Varret, R. Boese, L. Zsolnai, G. Huttner, D. Astruc, *Organometallics* **1992**, *11*, 1454–1456.

[17] P. L. Holland, R. A. Andersen, R. G. Bergmann, *Organometallics* **1998**, *17*, 433–437.

[18] C. Elschenbroich, M. Wolf, O. Schiemann, K. Harms, O. Burghaus, J. Pebler, *Organometallics* **2002**, *21*, 5810–5819.

[19] C. Reichardt, *Solvents and Solvent Effects in Organic Chemistry*, 1st reprint of the 2nd ed., VCH, Weinheim, **1990**.

[20] a) J. L. Oudar, D. S. Chemla, *J. Chem. Phys.* **1977**, *66*, 2664–2668; b) J. L. Oudar, *J. Chem. Phys.* **1977**, *67*, 446–457.

[21] M. Rosenblum, *Chemistry of the iron group metallocenes*, Wiley Interscience New York, **1965**, chapter 2.

[22] Y. S. Sohn, D. N. Hendrickson, H. B. Gray, *J. Am. Chem. Soc.* **1971**, *93*, 3603–3612.

[23] a) M. B. Robin, P. Day, *Adv. Inorg. Radiochem.* **1967**, *10*, 247–422; b) C. Creutz, *Prog. Inorg. Chem.* **1983**, *30*, 1–73.

[24] O. V. Gusev, M. A. Ievlev, M. G. Peterleitner, S. M. Peregudova, L. I. Denisovich, P. V. Petrovskii, N. A. Ustynuyuk, *J. Organomet. Chem.* **1997**, *534*, 57–66.

[25] O. V. Gusev, M. G. Peterleitner, M. A. Ievlev, A. M. Kal'sin, P. V. Petrovskii, L. I. Denisovich, N. A. Ustynuyuk, *J. Organomet. Chem.* **1997**, *531*, 95–100.

[26] N. G. Conelly, W. E. Geiger, *Chem. Rev.* **1996**, *96*, 877–910.

[27] C. Patoux, C. Coudret, J.-P. Launay, C. Joachim, A. Goudron, *Inorg. Chem.* **1997**, *36*, 5037–5049.

[28] M. Iyoda, T. Kondo, T. Okabe, H. Matsuyama, S. Sasaki, Y. Kuwatani, *Chem. Lett.* **1997**, 35–36.

[29] K. Clays, A. Persoons, *Rev. Sci. Instrum.* **1992**, *63*, 3285–3289.

[30] S. Stadler, R. Dietrich, G. Bourhill, C. Bräuchle, A. Pawlik, W. Grahn, *Chem. Phys. Lett.* **1995**, *247*, 271–276.

[31] S. K. Kurtz, T. T. Perry, *J. Appl. Phys.* **1968**, *39*, 3798–3813.

[32] B. Bildstein, *Coord. Chem. Rev.* **2000**, *206–207*, 369–394.

[33] J. Zyss, J. L. Oudar, *Phys. Rev. A* **1982**, *26*, 2028–2048.

[34] J. W. Kang, K. Moseley, P. M. Maitlis, *J. Am. Chem. Soc.* **1969**, *91*, 5970–5977.

[35] a) R. A. Zelonka, M. C. Baird, *J. Organomet. Chem.* **1972**, *44*, 383–389; b) T. A. Stephenson, D. A. Tocher, *Organomet. Synth.* **1986**, *3*, 99–103.

[36] W. A. Hermann, G. Brauer, *Synthetic Methods of Organometallic and Inorganic Chemistry*, Thieme Verlag, Stuttgart, **1996**, vol. 1, p. 12.

[37] K. Jonas, P. Klusmann, R. Goddard, *Z. Naturforsch., Teil B* **1995**, *50*, 394–404.

[38] a) G. M. Sheldrick, *SHELXS-86 Program for crystal structure determination*, University of Göttingen, Germany, **1986**; b) G. M. Sheldrick, *SHELXL-97 Program for crystal structure refinement*, University of Göttingen, Germany, **1997**.

[39] P. v. Sluis, A. L. Spek, *Acta Crystallogr., Sect. A* **1990**, *46*, 194.

[40] M. H. Garcia, J. C. Rodrigues, A. Romão Dias, M. F. M. Piedade, M. T. Duarte, M. P. Robalo, N. Lopes, *J. Organomet. Chem.* **2001**, *632*, 133–144.

[41] R. W. Terhune, P. D. Maker, C. M. Savage, *Phys. Rev. Lett.* **1965**, *14*, 681.

[42] C. Dehu, F. Meyers, E. Hendrickx, K. Clays, A. Persoons, S. R. Marder, J. L. Bredas, *J. Am. Chem. Soc.* **1995**, *117*, 10127–10128.

[43] S. Stadler, R. Dietrich, G. Bourhill, C. Bräuchle, A. Pawlik, W. Grahn, *Chem. Phys. Lett.* **1995**, *247*, 271–276; T. Farrell, T. Meyer-Friedrichsen, M. Malessa, C. Wittenburg, J. Heck, A. R. Manning, *J. Organomet. Chem.* **2001**, *625*, 32–39; T. Farrell, A. R. Manning, G. Mitchell, J. Heck, T. Meyer-Friedrichsen, M. Malessa, C. Wittenburg, M. H. Prosenc, D. Cunningham, P. McArdle, *Eur. J. Inorg. Chem.* **2002**, 1677–1686.

[44] Paralite Optical Parametrical Oscillator, LAS GmbH.

[45] T. Kodaira, A. Watanabe, O. Ito, M. Matsuda, K. Clays, A. Persoons, *J. Chem. Soc., Faraday Trans.* **1997**, *93*, 3039–3044.

[46] C. Lambert, G. Nöll, E. Schmälzlin, K. Meerholz, C. Bräuchle, *Chem. Eur. J.* **1998**, *4*, 2129–2135.

[47] C. Lambert, W. Gaschler, E. Schmälzlin, K. Meerholz, C. Bräuchle, *J. Chem. Soc., Perkin Trans. 2* **1999**, 577–587.

Received: September 14, 2005
Published Online: December 22, 2005

